PROTON RADIOACTIVITY — SPHERICAL AND DEFORMED* **

C.N. Davids[a], P.J. Woods[b], D. Seweryniak[a,c], A.A. Sonzogni[a], J.C. Batchelder[d], C.R. Bingham[e], T. Davinson[b], D.J. Henderson[a], R.J. Irvine[b], G.L. Poli[f], J. Uusitalo[a] and W.B. Walters[c]

[a] Physics Division, Argonne National Laboratory, Argonne, IL 60439, USA
[b] University of Edinburgh, Edinburgh, EH9 3JZ, United Kingdom
[c] Dept. of Chemistry, Univ. of Maryland, College Park. MD 20742, USA
[d] UNIRIB, Oak Ridge Associated Universities, Oak Ridge, TN 37831, USA
[e] Dept. of Phys. and Astron., Univ. of Tennessee, Knoxville, TN 37996, USA
[f] Istituto Fisica Generale Applicata, University of Milano, I-20133 Milano, Italy

(Received January 13, 1999)

The proton drip line defines one of the fundamental limits to nuclear stability. Nuclei lying beyond this line are energetically unbound to the emission of a constituent proton from their ground states. This phenomenon is known as proton radioactivity. For near-spherical nuclei in the region of the drip line between $Z = 69$ (Tm) and $Z = 81$ (Tl), proton decay transition rates have been shown to be well reproduced by WKB calculations using spectroscopic factors derived from a low-seniority shell model calculation. Another approach using spectroscopic factors obtained from the independent quasiparticle approximation has also proved successful in this region. These interpretations have allowed the extraction of nuclear structure information from nuclei well beyond the proton drip line. The rare-earth proton emitters ^{141}Ho and ^{131}Eu have recently been observed, and their decay rates can only be explained by assuming large deformation for these nuclei. In addition to providing information on the wavefunctions and deformations of these nuclei, these results offer the opportunity to study the phenomenon of quantum mechanical tunneling through a deformed potential barrier.

PACS numbers: 23.50.+z, 21.10.Re, 21.10.Tg, 27.60.+j

* Presented at the XXXIII Zakopane School of Physics, Zakopane, Poland, September 1–9, 1998.

** Work supported by the U.S. Department of Energy, Nuclear Physics Division, under Contract No. W-31-109-ENG-38.

1. Introduction

The proton drip-line defines one of the fundamental limits to nuclear stability. Nuclei lying beyond this locus are energetically unbound to the emission of a constituent proton from their ground states [1]. For heavy nuclei ($Z > 50$) the presence of a large Coulomb barrier reduces the proton barrier penetration probability to the extent that proton decays of nuclei from their ground states have measurably long half-lives. Figure 1 shows

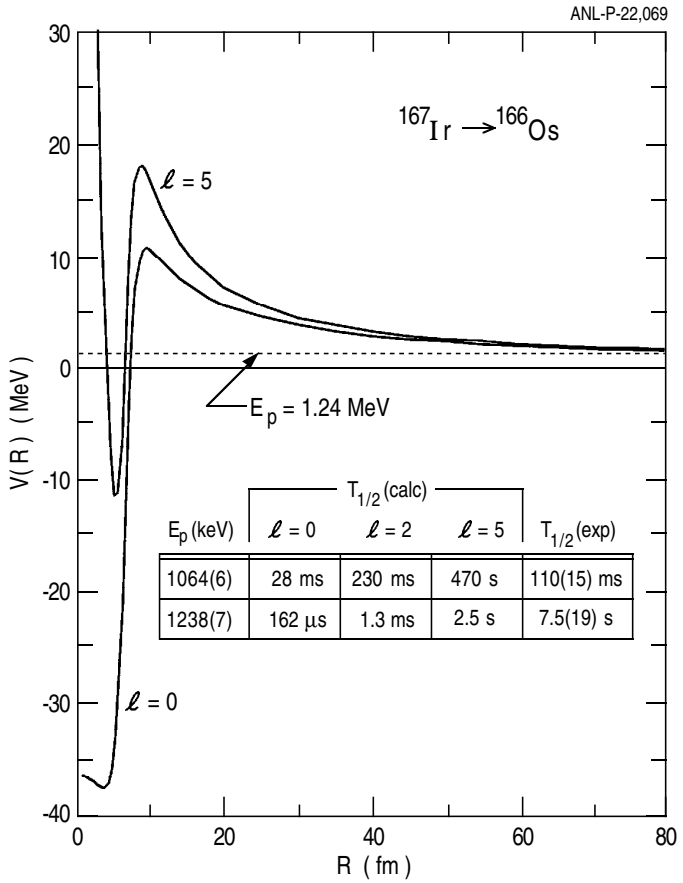

Fig. 1. Potential between the proton and the daughter nucleus calculated for the proton decay of ^{167}Ir.

the potential between the proton and the daughter nucleus calculated for the proton decay of ^{167}Ir using the real part of the Becchetti-Greenlees optical potential [2]. Figure 2 shows the calculated half-lives for ^{167}Ir decay protons emitted from the $0h_{11/2}$, $1d_{3/2}$, and $2s_{1/2}$ orbitals, carrying off 5, 2, and 0

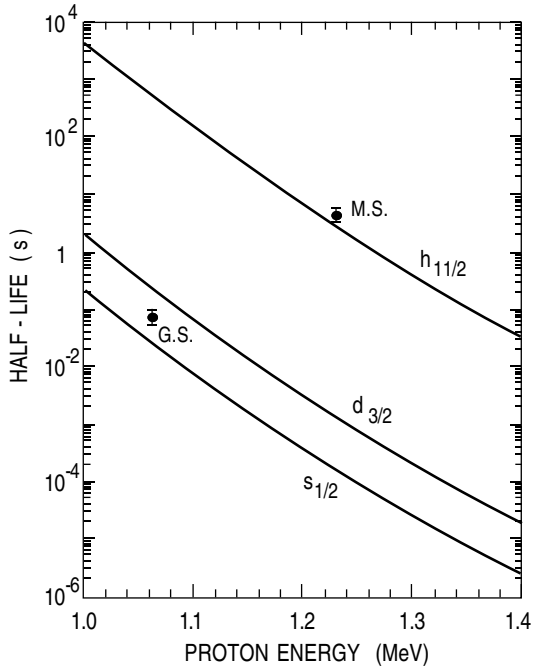

Fig. 2. Calculated half-lives for ^{167}Ir decay protons emitted from the $0h_{11/2}$, $1d_{3/2}$, and $2s_{1/2}$ orbitals.

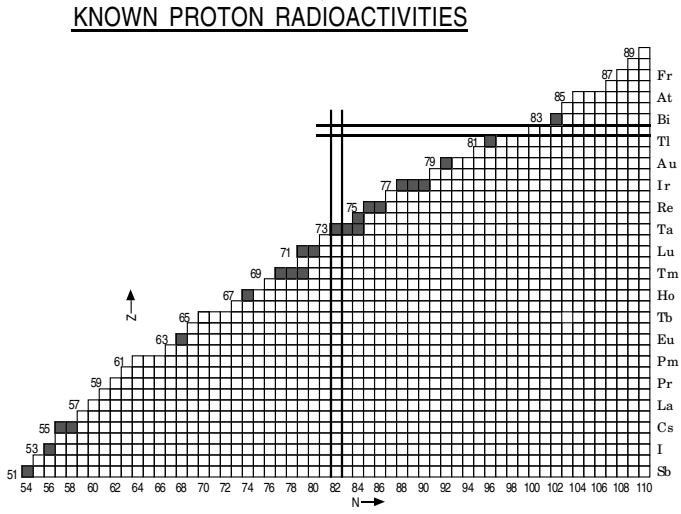

Fig. 3. N-Z plot of the known proton emitters.

units of angular momentum, respectively. The figure clearly demonstrates the high degree of sensitivity of the partial half-life $t_{1/2,p}$ to the orbital angular momentum ℓ_p of the emitted proton. This is due to the relatively low mass of the proton compared to that for an alpha particle.

Figure 3 shows the landscape of known proton emitters for $Z > 50$. For near-spherical nuclei in the region of the drip-line between $Z = 69$ (Tm) and $Z = 81$ (Tl), proton decay transition rates have been shown to be well reproduced by WKB calculations using spectroscopic factors derived from a low-seniority spherical shell-model calculation [3]. This model considers the proton configuration to have a closed core at $Z = 64$, with degenerate $0h_{11/2}$, $1d_{3/2}$, and $2s_{1/2}$ Fermi levels filling up to $Z = 82$, and the neutrons behaving as spectator particles. More sophisticated theoretical approaches using spectroscopic factors based on the independent quasiparticle approximation have also obtained similarly good agreement for this region, provided spherical configurations are assumed [4].

In the region of the proton drip-line below $Z = 69$, the macroscopic-microscopic mass model of Möller *et al.* [5] predicts the onset of large prolate deformations ($\beta_2 \sim 0.3$). It is of great theoretical interest to investigate proton decay transition rates in this region. For deformed nuclei ℓ_p is no longer a good quantum number in the parent nucleus, and significant departures from spherical decay rate calculations would provide a signature for the onset of deformation. Anomalous proton decay rates measured for the isotopes ^{109}I and ^{113}Cs [6] have been shown to be consistent with calculations assuming relatively small deformations ($\beta_2 \sim 0.1$) [7]. Proton decay rates from highly deformed nuclei will provide a challenging test for theoretical descriptions of this process. Working toward that end, we have recently observed the rare-earth proton emitters ^{141}Ho and ^{131}Eu [8]. The decay rates for these nuclei have been reproduced by assuming large deformation for these nuclei.

2. Experimental method

The proton emitters described in this paper were observed at the ATLAS heavy ion accelerator facility at Argonne National Laboratory. Heavy ion beams with typical intensities of a few particle nanoamperes were used to bombard targets of thickness 0.5-1.0 mg/cm^2. Reaction products entered the Fragment Mass Analyzer (FMA) [9] where they are separated from the primary beam and dispersed in mass/charge (M/Q) at the focal plane. A position-sensitive parallel grid avalanche counter (PGAC) located at the focal plane provided M/Q, time of arrival, and energy-loss signals of the recoiling nuclei. After traversing this detector the ions traveled a further 47 cm before being implanted into a double-sided silicon strip detector (DSSD) of thickness 65 μm, area 16 x 16 mm^2, and having 48 orthogonal strips on the front and rear respectively [10].

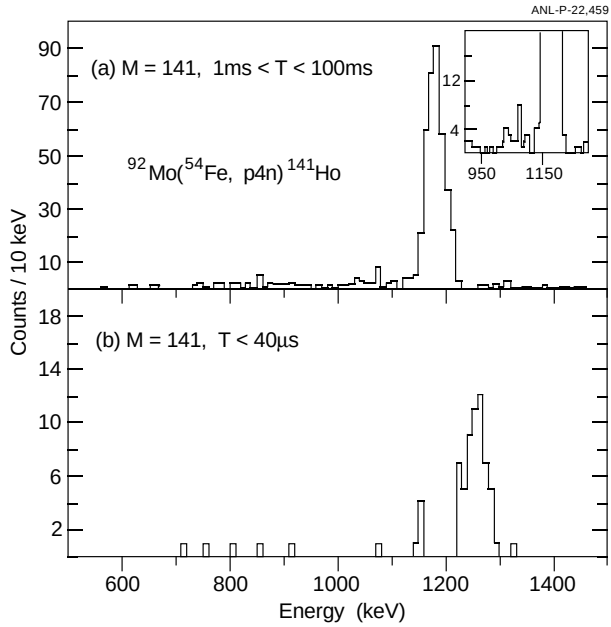

Fig. 4. Energy spectrum of protons from the decay of ^{141}Ho.

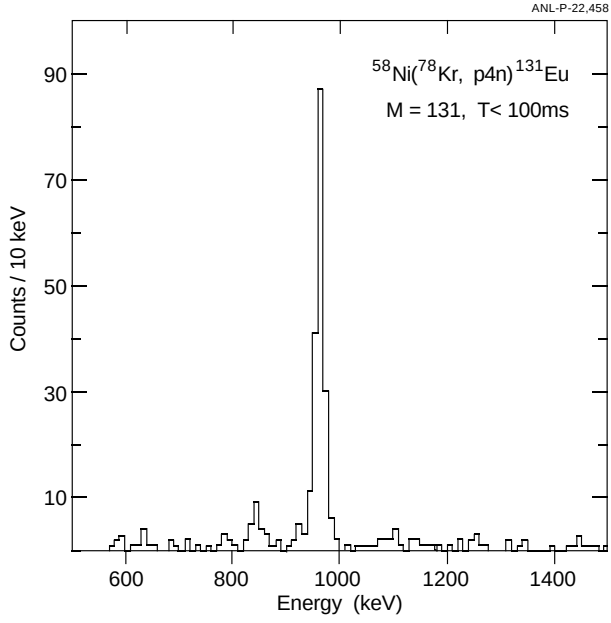

Fig. 5. Energy spectrum of protons from the decay of ^{131}Eu.

As an example, figure 4 shows the energy spectrum of decay events occurring within 25 ms of an $A = 141$ recoil implanted in the same DSSD pixel. The reaction used was 285 MeV ^{54}Fe on ^{92}Mo. A peak is clearly visible at an energy of 1169(8) keV. The low decay energy rules out α radioactivity, and this peak is assigned to proton radioactivity from ^{141}Ho, produced with a cross section $\sigma \sim 250$ nb. The known ground-state proton decay line of ^{147}Tm ($E_p = 1051(4)$ keV) was used to calibrate the energy of this line. The measured Q-value of 1177(8) keV for ^{141}Ho is in excellent agreement with the 1.15 MeV prediction of the Liran–Zeldes shell-model based mass formula [11], which is known to reproduce proton decay Q-values in this region very well. The half-life of the proton transition was determined to be 4.2(4) ms, which is considerably shorter than the predicted β^+-decay half-life of 271 ms [12]. Therefore, we assume that the proton decay branch $b_p \approx 100\%$.

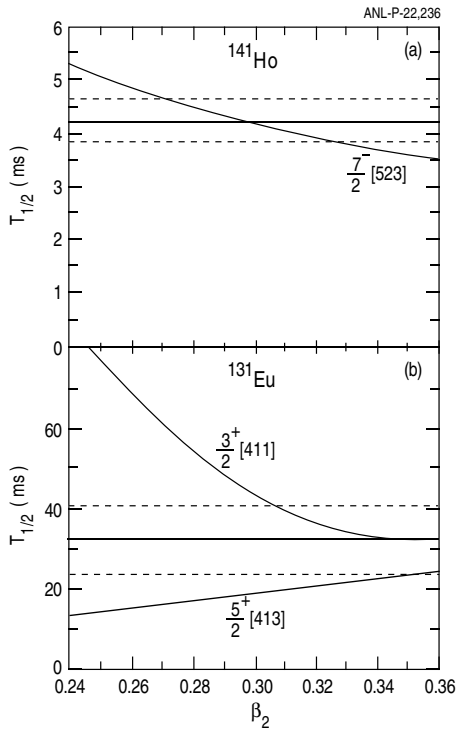

Fig. 6. (a) — Calculated proton decay half-life for ^{141}Ho based on the $7/2^-[523]$ Nilsson orbital. The observed half-life lies in the band between the dashed lines. (b) — Calculated proton decay half-life for ^{131}Eu based on the $3/2^+[411]$ and $5/2^+[413]$ Nilsson orbitals. The observed half-life lies in the band between the dashed lines. Pairing has been neglected in both (a) and (b).

A beam of ^{40}Ca ions was used to bombard a ^{96}Ru target in order to produce ^{131}Eu nuclei. Figure 5 shows the energy spectrum of decays occurring within 150 ms of an $A = 131$ recoil implanted into the same DSSD pixel. The peak at an energy of 950(8) keV is assigned to the proton decay of ^{131}Eu, produced with a cross section $\sigma \sim 90$ nb. This corresponds to a proton decay Q-value of 957(8) keV, which compares well with the predicted value of 1.08 MeV from the Liran–Zeldes mass formula [11]. The observed half-life of ^{131}Eu is 26(6) ms which, when combined with the predicted β^+-decay half-life of 147 ms [12], yields a derived partial proton half-life of 32(9) ms.

3. Results

Spherical WKB calculations for ^{141}Ho using the Becchetti-Greenlees optical potential [2] and a spectroscopic factor of 0.89 derived from the low-seniority spherical shell-model calculations of ref. [3] predict half-lives of 1 μs, 10 μs, and 37 ms for the $2s_{1/2}$, $1d_{3/2}$ and $0h_{11/2}$ proton orbitals, respectively. It is clear that none of these orbitals can explain the observed 4.2(4) ms half-life of ^{141}Ho. Since the major assumption in these calculations is that the nucleus is spherical or nearly spherical, this strongly suggests that ^{141}Ho is highly deformed. A number of calculations point to the presence of deformation in this region. The macroscopic–microscopic mass model [5] predicts that a rapid transition between near spherical and highly deformed shapes takes place between Tm and Ho isotopes in this region of the proton drip-line. A ground-state prolate deformation of $\beta_2 = 0.29$ is calculated for ^{141}Ho. Recent deformed Hartree-Fock calculations for proton-rich nuclei also predict a high deformation $\beta_2 = +0.33$ for the neighboring even-Z nucleus ^{138}Dy [13]. In addition, Ω_p^π, the angular momentum projection on the nuclear symmetry axis for the odd proton, is predicted by Möller *et al.* to be $7/2^-$ [12], corresponding to the $7/2^-[523]$ Nilsson configuration. This same configuration is observed for the deformed ground states of odd-A Ho isotopes with $N > 88$ [14]. Another possibility for the odd proton in ^{141}Ho is the nearby $1/2^+[411]$ orbital.

The predictions of Möller *et al.* place ^{131}Eu in the middle of the region of high prolate deformation with $\beta_2 = 0.33$ and an Ω_p^π value of $3/2^+$, corresponding to a $3/2^+[411]$ configuration for the ground state [5,12]. However, the nearby $5/2^+[413]$ and $5/2^-[532]$ Nilsson levels are also possibilities. In fact, the $5/2^+[413]$ configuration has been assigned to the ground states of all of the deformed odd-A Eu isotopes with $N > 88$ where known [14]. If ^{131}Eu had a spherical ground-state configuration the odd proton would occupy either a $1d_{5/2}$ or $0g_{7/2}$ state lying immediately below the $Z = 64$ shell closure. A low-seniority shell model calculation of the type successfully ap-

plied to the nuclei above the $Z = 64$ shell closure would imply spectroscopic factors of 1/3 or 1/7 for the $1d_{5/2}$ state, and 1/4 or 1/7 for the $0g_{7/2}$ state, depending on whether a subshell or supershell model space is assumed. This would give WKB half-life predictions $\sim$1 ms for the $1d_{5/2}$ state and a few hundred ms for the $0g_{7/2}$ state, neither of which is consistent with the measured value. Again the failure of these calculations can be attributed to the expected strong deformation of ^{131}Eu.

We have calculated the partial proton decay rates of ^{141}Ho and ^{131}Eu using the formalism for the proton decay of deformed nuclei developed by Bugrov and Kadmenskii [7,15,16]. This model was first developed to account for the anomalous proton decay rates of ^{109}I and ^{113}Cs, which were thought to be due to the influence of small deformations ($\beta_2 \sim 0.1$) in that region [6, 7]. Their model treats the axially-symmetric deformed odd-A decay parent as an inert core plus an odd proton in a quasi-bound state. It can be shown that their approach is equivalent to the DWBA method of Ref. [4], adapted to deformed nuclei.

Proton partial half-lives have been calculated for the decays of ^{141}Ho and ^{131}Eu, for β_2-values between 0.25 and 0.35. Half-lives have been calculated for ^{141}Ho assuming that the odd proton occupies the $7/2^-[523]$ and $1/2^+[411]$ Nilsson orbitals, and for ^{131}Eu assuming the $3/2^+[411]$, $5/2^+[413]$, and $5/2^-[532]$ orbitals. For ^{141}Ho, the $1/2^+[411]$ case is ruled out because the calculated half-lives are in the vicinity of 15 μs, and for ^{131}Eu the $5/2^-[532]$ case is ruled out because the calculated half-lives are greater than 0.5 s. In these calculations, we have neglected both the effects of pairing in the daughter wavefunction, and possible small shape differences between parent and daughter nuclei. Incorporating pairing increases the calculated half-lives by roughly a factor of two.

Figures 6(a) and (b) show the calculated proton partial half-lives for ^{141}Ho and ^{131}Eu as a function of deformation. The $7/2^-[523]$ calculations for ^{141}Ho are consistent with the observed half-life over a wide range of high β_2 values. In the case of ^{131}Eu, good agreement is obtained using the $3/2^+[411]$ configuration with a deformation $\beta_2 \geq 0.3$. This is consistent with the predictions of Möller *et al.* [5, 12], which indicate a $3/2^+[411]$ ground-state configuration with a corresponding deformation $\beta_2 = +0.33$. However, it can be seen from figure 6 that the $5/2^+[413]$ configuration also gives reasonable agreement for high deformations, and cannot be ruled out as a possibility.

A close look at figure 5 indicates the presence of a small proton group about 120 keV lower in energy than the main group. We interpret this as a proton transition from the ground state of ^{131}Eu to the first excited 2^+ state in the daughter nucleus ^{130}Sm. Calculations of the decay rate of this transition are currently in progress [17].

The authors would like to thank D. Kurath, R. L. Chasman, H. Esbensen, M. Peshkin, and J. Cizewski for valuable discussions. P. J. W. and T. D. wish to acknowledge travel support from NATO under Grant No. CRG 940303. R. J. I. would like to thank EPSRC for support.

REFERENCES

[1] P.J. Woods, C.N. Davids, *Annu. Rev. Nucl. Part. Sci.* **47**, 541 (1997).

[2] F. D. Becchetti, G. W. Greenlees, *Phys. Rev.* **182**, 1190 (1969).

[3] C.N. Davids *et al.*, *Phys. Rev.* **C 55**, 2255 (1997).

[4] S. Åberg, P.B. Semmes, W. Nazarewicz, *Phys. Rev.* **C 56**, 1762 (1997).

[5] P. Möller, J. R. Nix, W. D. Myers, W. J. Swiatecki, *At. Data Nucl. Data Tables* **59**, 185 (1995).

[6] A. Gillitzer, T. Faestermann, K. Hartel, P. Kienle, E. Nolte, *Z. Phys.* **A326**, 107 (1987).

[7] V. P. Bugrov, S. G. Kadmenskii, *Sov. J. Nucl. Phys.* **49**, 967 (1989).

[8] C.N. Davids *et al.*, *Phys. Rev. Lett.* **80**, 1849 (1998).

[9] C. N. Davids, B. B. Back, K. Bindra, D. J. Henderson, W. Kutschera, T. Lauritsen, Y. Nagame, P. Sugathan, A. V. Ramayya, W. B. Walters, *Nucl. Instrum. Methods* **B70**, 358 (1992).

[10] P. J. Sellin, *et al.*, *Nucl. Instrum. Methods* **A311**, 217 (1992).

[11] S. Liran, N. Zeldes, *At. Data Nucl. Data Tables* **17**, 431 (1976).

[12] P. Möller, J. R. Nix, K.-L. Kratz, *At. Data Nucl. Data Tables* **66**, 131 (1997).

[13] N. Tajima, N. Onishi, S. Takahara, *Nucl. Phys.* **A588**, 215c (1995).

[14] *Eighth Edition of the Table of Isotopes*, R. B. Firestone, ed. V. S. Shirley, Wiley, 1996.

[15] D. D. Bogdanov, V. P. Bugrov, S. G. Kadmenskii, *Sov. J. Nucl. Phys.* **52**, 229 (1990).

[16] S. G. Kadmenskii, V. P. Bugrov, *Phys. of Atomic Nuclei* **59**, 399 (1996).

[17] A. A. Sonzogni *et al.*, in preparation (1998).